Autonomous Distribution of Programmable Multiqubit Entanglement in a Dual-Rail Quantum Network

J. Agustí,[1,2,3] X. H. H. Zhang,[1,2,3] Y. Minoguchi,[4] and P. Rabl[1,2,3,4]

[1]*Technical University of Munich, TUM School of Natural Sciences, Physics Department, 85748 Garching, Germany*
[2]*Walther-Meißner-Institut, Bayerische Akademie der Wissenschaften, 85748 Garching, Germany*
[3]*Munich Center for Quantum Science and Technology (MCQST), 80799 Munich, Germany*
[4]*Vienna Center for Quantum Science and Technology, Atominstitut, TU Wien, 1020 Vienna, Austria*

(Received 7 July 2023; accepted 25 November 2023; published 18 December 2023)

We propose and analyze a scalable and fully autonomous scheme for preparing spatially distributed multiqubit entangled states in a dual-rail waveguide QED setup. In this approach, arrays of qubits located along two separated waveguides are illuminated by correlated photons from the output of a nondegenerate parametric amplifier. These photons drive the qubits into different classes of pure entangled steady states, for which the degree of multipartite entanglement can be conveniently adjusted by the chosen pattern of local qubit-photon detunings. Numerical simulations for moderate-sized networks show that the preparation time for these complex multiqubit states increases at most linearly with the system size and that one may benefit from an additional speedup in the limit of a large amplifier bandwidth. Therefore, this scheme offers an intriguing new route for distributing ready-to-use multipartite entangled states across large quantum networks, without requiring any precise pulse control and relying on a single Gaussian entanglement source only.

DOI: 10.1103/PhysRevLett.131.250801

Introduction.—As quantum computing and quantum communication systems with an increasing number of coherently integrated components become technologically available, a growing demand for efficient schemes to transfer quantum states or distribute entanglement across different parts of such networks will arise [1–4]. While basic protocols to do so are well known and have already been successfully implemented in a variety of platforms [5–14], it is envisioned that in future quantum devices, entanglement must be generated and interchanged among many thousands of qubits within a limited coherence time. In view of this challenge, there is a strong motivation to go beyond a serial application of existing protocols and search for more efficient quantum communication strategies that are fast, parallelizable, and, ideally, require a minimal amount of classical control.

In this Letter, we describe a fully autonomous entanglement distribution scheme, which exploits an intriguing physical effect, namely the formation of multipartite entangled stationary states in a cascaded dual-rail quantum network. Specifically, we consider a configuration as shown in Fig. 1, where spatially separated qubits located along two photonic waveguides are illuminated by the correlated output of a nondegenerate parametric amplifier [15]. Previously, it was proposed to use broadband squeezed reservoirs for generating bipartite entanglement between separated qubit pairs [16–22] or, for specific arrangements, between qubits along a 1D channel [23,24] or in coupled arrays [25,26]. Here we show, first of all, that this concept can be generalized to produce, under ideal conditions, an arbitrary number of maximally entangled qubit pairs over large distances. Moreover, we find that the entanglement shared between different sets of qubits can be adjusted by simply changing the local qubit-photon detunings. This provides a convenient way to "program" different classes of multipartite entangled states without the need for any time-dependent control or additional nonlocal operations.

To evaluate the scalability of this approach, we simulate the formation of these multipartite entangled states under

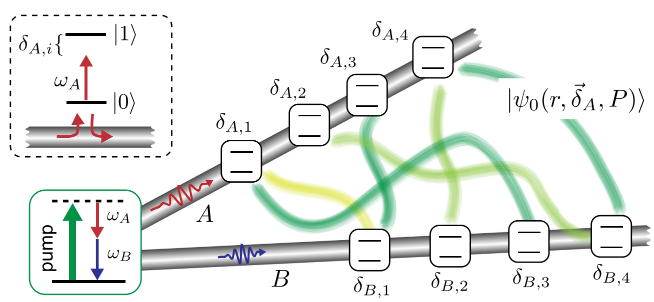

FIG. 1. Sketch of a dual-rail quantum network, where qubits along two separated waveguides are driven by the correlated output of a nondegenerate parametric amplifier and relax into a pure steady state $|\psi_0(r,\vec{\delta}_A,P)\rangle$. As shown in the inset, the qubits in waveguide A (B) are detuned from the central photon frequency ω_A (ω_B) by $\delta_{A,i}$ ($\delta_{B,i}$) and the qubit-waveguide coupling is assumed to be fully directional. See text for more details.

more realistic conditions, taking in particular a finite bandwidth of the squeezing source into account. We find that the maximal number of entangled qubit pairs $N_{\rm ent}$ remains rather robust under the influence of experimental imperfections, and that the total preparation time $T_{\rm prep} \sim N_{\rm ent}$ scales at most linearly with the system size, independently of the complexity of the prepared state. In the limit of a large amplifier bandwidth, the intrinsic parallelization of the preparation scheme can be exploited to further reduce $T_{\rm prep}$, which shifts the technological requirements for scalability from the control of many qubits to the optimization of a single Gaussian squeezing source. This can be advantageous for many applications in optical, microwave, or hybrid [27–30] quantum networks, where such photonic devices are currently developed [14,31–37].

Model.—We consider a dual-rail quantum network as depicted in Fig. 1, where two sets of qubits $\eta = A, B$ are coupled to two separate photonic channels. The waveguides are connected to a common nondegenerate parametric amplifier, which we model by a two-mode squeezing interaction ($\hbar = 1$) $H_\chi = ig(a_A^\dagger a_B^\dagger - a_A a_B)$ for two local modes with bosonic annihilation operators a_A and a_B. These photons then decay into the respective waveguides with rate κ and drive the qubits into a correlated state. For the following analysis, we assume that the qubit-waveguide coupling is fully directional [38–40] and label the qubits by the index $i = 1, \ldots, N$ along the direction of propagation. Such conditions can be realized by using circulators [41–46], chiral waveguides [40], or other schemes for directional coupling [47–50].

We first focus on the limit of a broadband amplifier, $\kappa \to \infty$, in which case the dynamics of the photons can be adiabatically eliminated to obtain an effective master equation (see Ref. [51] for more details)

$$\dot{\rho}_{\rm q} = -i[H_{\rm casc}, \rho_{\rm q}] + \sum_{\eta=A,B} \gamma \mathcal{D}[J_\eta]\rho_{\rm q} \tag{1}$$

for the reduced qubit density operator $\rho_{\rm q}$. Here γ denotes the decay rate of each individual qubit and $\mathcal{D}[C]\rho = C\rho C^\dagger - \{C^\dagger C, \rho\}/2$. In Eq. (1) we have already rewritten the underlying directional qubit-qubit interactions in terms of a coherent Hamiltonian evolution with

$$H_{\rm casc} = \sum_{\eta,i} \frac{\delta_{\eta,i}}{2}\sigma^z_{\eta,i} + i\frac{\gamma}{2}\sum_{\eta,j>i}(\sigma^+_{\eta,i}\sigma^-_{\eta,j} - {\rm H.c.}), \tag{2}$$

and purely dissipative processes with collective jump operators

$$J_A = \cosh(r)L_A - \sinh(r)L_B^\dagger, \tag{3}$$

$$J_B = \cosh(r)L_B - \sinh(r)L_A^\dagger, \tag{4}$$

where $L_\eta = \sum_{i=1}^N \sigma^-_{\eta,i}$. In this broadband limit, the system is thus fully determined by the squeezing parameter $r = 2\tanh^{-1}(2g/\kappa)$, characterizing the degree of two-mode squeezing of the photon source, and the two sets of qubit detunings, $\vec{\delta}_{\eta=A,B} = (\delta_{\eta,1}, \delta_{\eta,2}, \ldots, \delta_{\eta,N})$.

Steady states.—Equation (1) describes an open quantum many-body system with competing coherent and dissipative processes, which in general drive the qubits into a highly mixed steady state. However, in the following, we show that there exist specific conditions under which the steady state of the network $\rho_{\rm q}^0 = |\psi_0\rangle\langle\psi_0|$ is not only pure but also exhibits different degrees of multipartite entanglement that can be controlled by the local detunings $\delta_{\eta,i}$.

We start our analysis by considering the simplest case of a single pair of qubits ($N = 1$) and $\delta_{A,1} = \delta_{B,1} = 0$, as originally discussed in Ref. [16]. In this case, one can explicitly show that the unique steady state of Eq. (1) is $|\psi_0\rangle = |\Phi^+_{1,1}\rangle$, where

$$|\Phi^+_{i,j}\rangle = \frac{\cosh(r)|0_{A,i}\rangle|0_{B,j}\rangle + \sinh(r)|1_{A,i}\rangle|1_{B,j}\rangle}{\sqrt{\cosh(2r)}} \tag{5}$$

approaches a maximally entangled Bell state for $r \gg 1$. This state satisfies the dark-state conditions $J_\eta|\psi_0\rangle = 0$ and $H_{\rm casc}|\psi_0\rangle = 0$, which implies that once the qubits have reached the steady state, they completely decouple from the squeezed photonic bath. Consequently, they no longer affect successive qubits along the waveguide.

Importantly, this observation remains true even for finite detunings satisfying $\delta_{A,1} + \delta_{B,1} = 0$, which then allows us to systematically identify also more complex multiqubit steady states by proceeding in two steps. First, we set $\vec{\delta}_B = -\vec{\delta}_A$, such that, according to the argument from above, qubits with the same index decouple pairwise from the photonic reservoir. The network then relaxes into the pure steady state $|\psi_0\rangle = |\Phi_\parallel\rangle$, where

$$|\Phi_\parallel\rangle = \bigotimes_{i=1}^N |\Phi^+_{i,i}\rangle \tag{6}$$

is the product of N consecutive Bell pairs of the type given in Eq. (5). Interestingly, this result is independent of the total number of qubit pairs, similar to what has been found for coupled spin chains [26] or discrete cavity arrays [25].

In the second step, we make use of the form invariance of the cascaded master equation in Eq. (1) under unitary transformations of the type [38]

$$U_{i,i+1} = e^{i\theta_{i,i+1}(\vec{s}_{B,i}+\vec{s}_{B,i+1})^2}, \tag{7}$$

where $\vec{s}_\mu = (\sigma^x_\mu, \sigma^y_\mu, \sigma^z_\mu)/2$ and the mixing angle satisfies $\tan(\theta_{i,i+1}) = (\delta_{B,i} - \delta_{B,i+1})/\gamma$. Under these transformations, one finds that $U_{i,i+1}J_\eta U^\dagger_{i,i+1} = J_\eta$ and

$$U_{i,i+1} H_{\rm casc}(\vec{\delta}_A, \vec{\delta}_B) U_{i,i+1}^\dagger = H_{\rm casc}(\vec{\delta}_A, P_{i,i+1}\vec{\delta}_B), \quad (8)$$

where the permutation $P_{i,i+1}$ exchanges $\delta_{B,i}$ and $\delta_{B,i+1}$. In other words, given a pure steady state $|\psi_0\rangle$ for a certain detuning pattern $\vec{\delta}_B$, the state $|\psi_0'\rangle = U_{i,i+1}|\psi_0\rangle$ is a pure steady state of the same network with a permuted pattern of detunings, $\vec{\delta}_B' = P_{i,i+1}\vec{\delta}_B$.

This form invariance now allows us to construct a large family of multipartite entangled steady states, which are parametrized by (i) the squeezing parameter r, (ii) the set of detunings $\vec{\delta}_A$ for qubits in waveguide A, and (iii) a permutation P that fixes the detunings in waveguide B to be $\vec{\delta}_B = -P\vec{\delta}_A$. By decomposing $P = \prod_\sigma P_{i_\sigma, i_\sigma+1}$ into a product of nearest-neighbor transpositions, we can start with the state in Eq. (6) and then use the relation below Eq. (8) to derive an explicit expression for the corresponding steady state,

$$|\psi_0(r, \vec{\delta}_A, P)\rangle = \prod_\sigma U_{i_\sigma, i_\sigma+1}|\Phi_\parallel\rangle. \quad (9)$$

Importantly, this is also the unique steady state of the network, as discussed in more detail in [51]. A graphical illustration of Eq. (9) is presented in Fig. 2(a).

Entanglement.—To investigate the entanglement properties of the family of states in Eq. (9), we start with the case $N = 2$ and choose the only nontrivial permutation $P = P_{1,2}$. We obtain

$$|\psi_0\rangle = \frac{\gamma|\Phi^+_{1,1}\rangle|\Phi^+_{2,2}\rangle + i\Delta|\Phi^+_{1,2}\rangle|\Phi^+_{2,1}\rangle}{\sqrt{\gamma^2 + \Delta^2}}, \quad (10)$$

where $\Delta = \delta_{A,1} - \delta_{A,2}$. In Figs. 2(b) and 2(c) we visualize the entanglement structure of this state in terms of the concurrences $\mathcal{C}_{ij} \equiv \mathcal{C}(\rho_{A,i|B,j})$ [58,59] of the reduced bipartite qubit states $\rho_{A,i|B,j}$. For $\Delta = 0$, we find that for parallel pairs $\mathcal{C}_{ii} \simeq 1$ already for moderate values of $r \gtrsim 1$, consistent with the state $|\Phi_\parallel\rangle$. For $|\Delta| \gg \gamma$ the same is true for diagonal pairs, i.e., $\mathcal{C}_{12} = \mathcal{C}_{21} \simeq 1$. For all intermediate parameters, the state is a genuine four-partite entangled state [60] and belongs to the set of locally maximally entanglable states [61] for $r \gg 1$.

For a larger number of qubits, we can use the entanglement entropy $\mathcal{S}(\rho_r) = -\mathrm{Tr}\{\rho_r \ln \rho_r\}$ for a reduced state ρ_r to study the entanglement between different bipartitions of the network. First of all, this analysis shows that $\mathcal{S}_A \equiv \mathcal{S}(\rho_A) = -N \ln[x^x(1-x)^{(1-x)}]$, where $x = \cosh^2(r)/\cosh(2r)$ only depends on the squeezing parameter r. This can be understood from the fact that the unitaries $U_{i,i+1}$ only act within subsystem B. Thus, with respect to this partition, the states in Eq. (9) can be understood as generalized "rainbow states" [26,62,63] with

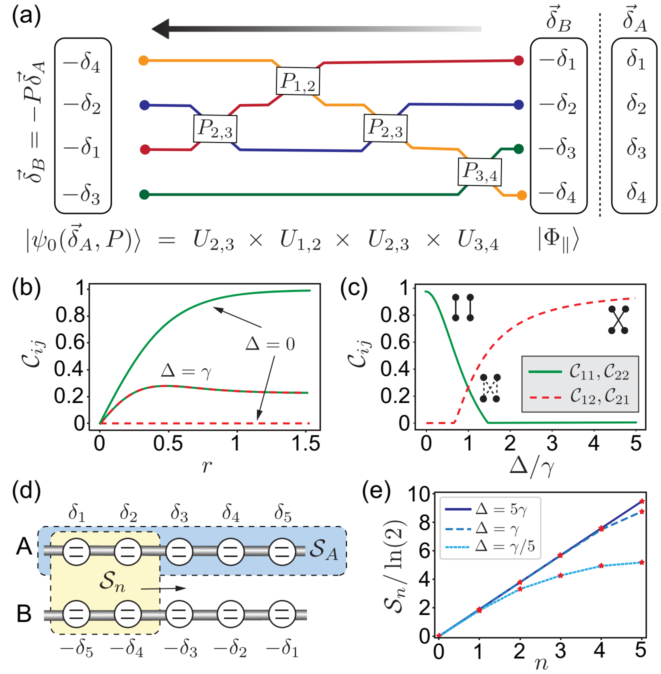

FIG. 2. (a) Graphical illustration of Eq. (9). Starting from $\vec{\delta}_B = -\vec{\delta}_A$, the detunings in waveguide B are reordered as $\vec{\delta}_B = -P\vec{\delta}_A$ through nearest-neighbor transpositions, following the colored lines as a guide to the eye. Each transposition maps into one of the unitary operations $U_{i,i+1}$ that determine the final steady state. (b) Bipartite entanglement expressed in terms of the concurrences $\mathcal{C}_{ij}$ for the four-qubit state in Eq. (10) as a function of r, and in (c) as a function of Δ for $r = 1$. (d) Sketch of the detuning pattern for the family of multipartite states described in the text and different partitions for evaluating the entanglement entropy. (e) Entanglement entropy $\mathcal{S}_n$ as a function of n, for different detunings Δ and $r = 1$.

a volume-law entanglement $\mathcal{S}(\rho_A) \simeq N \ln 2$ for $r \gtrsim 1$. In contrast, for partitions along the chain, the entanglement entropy $\mathcal{S}_n = \mathcal{S}(\rho_{[1,\ldots,n]})$ depends not only on the chosen permutation P but also on the pattern of detunings $\vec{\delta}_A$. This is illustrated in Figs. 2(d) and 2(e), where we consider as an example the detunings $\delta_{A,i} = (i-1)\Delta$ and the reversed order, $\delta_{B,i} = -P_{\rm rev}\delta_{A,i} = -\delta_{A,N+1-i}$, in waveguide B. For $\Delta \gg \gamma$ the unitaries in Eq. (9) correspond to approximate SWAP operations and $\mathcal{S}_n \simeq 2n \ln 2$. Instead, for $\Delta \lesssim \gamma$, the entangling unitaries $U_{i,i+1} \approx \sqrt{\mathrm{SWAP}}$ generate more multipartite entanglement across the whole chain, which reduces the block-entanglement $\mathcal{S}_n$ correspondingly. In general, different choices for $\vec{\delta}_A$ and P can be used to define certain blocks of qubits that are entangled among each other, independently of their physical location.

Preparation time.—So far we have shown that a single two-mode squeezing source is in principle enough to entangle an arbitrary number of qubits. However, for

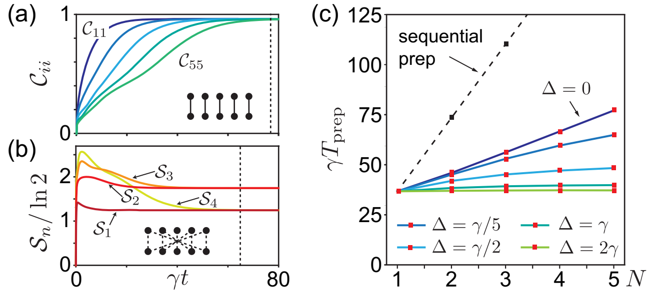

FIG. 3. (a) Relaxation into a bipartite entangled state for $\vec{\delta}_A = 0$ and (b) into a multipartite entangled state for $\vec{\delta}_B = -P_{\rm rev}\vec{\delta}_A$ and $\Delta = \gamma/5$. In both cases $N = 5$. (c) Scaling of the preparation time $T_{\rm prep}$ for different ratios Δ/γ, where $\delta_{A,i} = \Delta(i-1)$ and $\vec{\delta}_B = -\vec{\delta}_A$. We define $T_{\rm prep}$ via the condition $[1-\mu(T_{\rm prep})]/N = 0.001$, where $\mu = {\rm Tr}[\rho_q^2]$ is the purity. For the examples in (a) and (b), $T_{\rm prep}$ is indicated by the dashed vertical line. In all plots $r = 1$.

practical applications, we must still evaluate the time $T_{\rm prep}$ that it takes to prepare this state. To do so we first continue with the analysis of the ideal qubit master equation in Eq. (1) and study the relaxation dynamics toward the steady state $|\psi_0\rangle$, assuming that at $t = 0$ all qubits are initialized in state $|0\rangle$. In Fig. 3 this evolution is shown in (a) for the bipartite entangled state $|\Phi_\parallel\rangle$ with $\vec{\delta}_A = 0$ and in (b) for the multipartite entangled state considered in Fig. 2(e). In the bipartite case, we observe a successive, pairwise formation of Bell states with a total time $T_{\rm prep} \sim N$. Interestingly, already for $\delta_{A,i} = 0$, this preparation time is faster than a sequential preparation of N independent Bell pairs, i.e., $T_{\rm prep}(N) < NT_{\rm prep}(N=1)$. For detuned qubits the preparation time decreases further and $T_{\rm prep}(N) \simeq T_{\rm prep}(N=1)$ for $\Delta \gtrsim \gamma$, i.e., all pairs are prepared in parallel. For multipartite entangled states, where the differences $|\delta_{A,i} - \delta_{A,j}|$ are necessarily small, a full parallelization is not possible, but even in this case we obtain an intrinsic advantage compared to a sequential distribution of entanglement, followed by local gates. Note that for the same detunings $\vec{\delta}_A$, the relaxation time $T_{\rm prep}$ is independent of the permutation P.

Scalability.—All the results so far have been derived within the infinite-bandwidth approximation, which underlies Eq. (1) and assumes that correlated photons are available at arbitrary detunings. Obviously, this assumption must break down when $\delta_{\rm max} = \max\{|\delta_{A,i}|\} \gtrsim \kappa$, but even for $\delta_{A,i} = 0$ it has been shown that any finite κ limits the transferable entanglement [22]. Therefore, to provide physically meaningful predictions about the scalability of the current scheme it is necessary to go beyond the assumption of a Markovian squeezed reservoir [16–26] and take finite-bandwidth effects into account. To do so we now simulate the dynamics of the state of the full

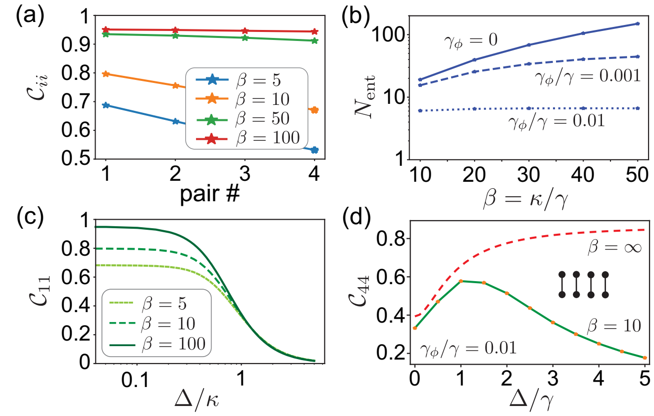

FIG. 4. (a) Plot of the steady-state concurrences $\mathcal{C}_{ii}$ for $\vec{\delta}_A = 0$ and different amplifier bandwidths. (b) Maximal number of entangled pairs, $N_{\rm ent}$ as a function of $\beta = \kappa/\gamma$, and different dephasing rates γ_ϕ. (c) Dependence of the concurrence of a single qubit pair on the detuning Δ, where $\delta_{A,1} = -\delta_{B,1} = \Delta$ and different values of β have been assumed. (d) Plot of the concurrence $\mathcal{C}_{44}$ in a chain of $N = 4$ qubit pairs with $\delta_{A,i} = (i-1)\Delta = -\delta_{B,i}$ and a finite dephasing rate. This plot illustrates the initial gain from a parallel preparation when $\Delta > 0$, while the entanglement decreases again when $\delta_{\rm max} = (N-1)\Delta \approx \kappa$, due to finite bandwidth effects. In all plots $r = 1$.

network ρ as described by the cascaded quantum master equation [51]

$$\dot{\rho} = -i[H_\chi, \rho] + \sum_\eta \kappa \mathcal{D}[a_\eta]\rho \\ \times \sum_{\eta,i}\left(-i\frac{\delta_{\eta,i}}{2}[\sigma^z_{\eta,i}, \rho] + \gamma\mathcal{D}[\sigma^-_{\eta,i}]\rho + \frac{\gamma_\phi}{2}\mathcal{D}[\sigma^z_{\eta,i}]\rho\right) \\ + \sum_{\eta,i}\sqrt{\kappa\gamma}\,\mathcal{T}[a_\eta, \sigma^-_{\eta,i}]\rho + \sum_{\eta,j>i}\gamma\mathcal{T}[\sigma^-_{\eta,i}, \sigma^-_{\eta,j}]\rho. \tag{11}$$

Here we have already included a finite dephasing rate γ_ϕ for each qubit and introduced the superoperator $\mathcal{T}[O_1, O_2]\rho = [O_1\rho, O_2^\dagger] + [O_2, \rho O_1^\dagger]$ to model directional interactions between all nodes along the same waveguide.

In Fig. 4(a) we plot the steady-state concurrences $\mathcal{C}_{ii}$ for the case $\delta_{A,i} = 0$ and different ratios $\beta = \kappa/\gamma$. We see that a finite bandwidth κ reduces the maximal amount of entanglement for the first pair [22] and also results in a gradual decay of the entanglement along the chain. By using a linear extrapolation, $N_{\rm ent} = \mathcal{C}_{11}/(\mathcal{C}_{11} - \mathcal{C}_{22})$, we can use these finite-size simulations to extract the maximal number of pairs that can be entangled for a given β and dephasing rate γ_ϕ. These results are summarized in Fig. 4(b). We see that for otherwise ideal conditions, rather large numbers of $N_{\rm ent} \sim 10$–100 can be entangled for moderate β, while the presence of dephasing or other imperfections sets additional limits on $N_{\rm ent}$. Note that these results are for $\delta_{A,i} = 0$, where the formation of the steady state is the slowest. Thus, these results represent approximate upper bounds for N_{ent} also for all other classes of multipartite entangled states. Additional plots for number of entangled pairs for various experimental sources of imperfections together with estimates for the achievable N_{ent} in state-of-the-art microwave networks are presented in [51].

Finally, let us return to the observed speedup for far-detuned qubits, but taking a finite amplifier bandwidth into account. In Fig. 4(c) we investigate, first of all, the dependence of $\mathcal{C}_{11}$ on the detuning $\delta_{A,1} = \Delta$. As expected, this plot shows a significant decay of the entanglement for $\Delta/\kappa > 1$, from which we also deduce that $\delta_{\max} < \kappa$ must be satisfied in the multiqubit case. Since for a parallel preparation with $T_{\mathrm{prep}}(\mathrm{N}) \sim \mathrm{const}$ we require $\delta_{\max} \approx \gamma N$, we conclude that the number of pairs that can be entangled in parallel $N_{\parallel} \approx N_{\mathrm{ent}}$ is actually comparable to the total number of entangled pairs for $\vec{\delta}_A = 0$. As a minimal illustration of this behavior, we consider in Fig. 4(d) the example of $N = 4$ pairs with $\delta_{A,i} = \Delta(i-1)$. We plot the concurrence of the last pair $\mathcal{C}_{44}$ for a fixed dephasing rate γ_ϕ and increasing detuning Δ. Up to $\Delta \sim \kappa$, entanglement increases due to a reduced preparation time, while for larger detunings finite-bandwidth effects set in and degrade the entanglement again. Note that for a parametric amplifier with asymmetric decay rates $\kappa_A \neq \kappa_B$, the structure of the ideal qubit master equation in Eq. (1) remains the same [51], but finite-bandwidth effects are determined by the minimal rate $\kappa_{\min} = \min\{\kappa_A, \kappa_B\}$.

Conclusions.—In summary, we have presented a fully autonomous scheme for distributing entanglement among two distant sets of qubits. Within the same setup, states with varying degrees of bi- and multipartite entanglement can be prepared by adjusting the squeezing strength and the local qubit detunings, while retaining a preparation time that scales at most linearly with N. Compared to related autonomous protocols discussed for single waveguides [23,24,38,39], locally coupled chains [25,26], or combinations thereof [64], the use of a propagating two-mode entangled source offers the possibility to entangle qubits that are arbitrarily far apart [51] and a systematic way to parallelize the scheme by increasing the bandwidth of the amplifier. This makes this approach very attractive for long-distance entanglement distribution schemes with long-lived spins or narrow-bandwidth optical emitters, but also for local area quantum networks [65–68], where multiple nodes can be simultaneously entangled with a limited amount of control.

We thank Aashish Clerk, Matthias Englbrecht, Tristan Kraft, Barbara Kraus, and Kirill Fedorov for many stimulating discussions. This work was supported by the European Union's Horizon 2020 research and innovation program under Grant Agreement No. 899354 (SuperQuLAN) and the Deutsche Forschungsgemeinschaft (DFG, German Research Foundation) No. 522216022. Most of the computational results presented were obtained using the CLIP cluster [69]. This research is part of the Munich Quantum Valley, which is supported by the Bavarian state government with funds from the Hightech Agenda Bayern Plus.

[1] J. I. Cirac, P. Zoller, H. J. Kimble, and H. Mabuchi, Quantum state transfer and entanglement distribution among distant nodes in a quantum network, Phys. Rev. Lett. **78**, 3221 (1997).

[2] T. E. Northup and R. Blatt, Quantum information transfer using photons, Nat. Photonics **8**, 356 (2014).

[3] A. Reiserer and G. Rempe, Cavity-based quantum networks with single atoms and optical photons, Rev. Mod. Phys. **87**, 1379 (2015).

[4] D. Awschalom, K. K. Berggren, H. Bernien, S. Bhave, L. D. Carr *et al.*, Development of quantum interconnects (QuICs) for next-generation information technologies, PRX Quantum **2**, 017002 (2021).

[5] D. L. Moehring, P. Maunz, S. Olmschenk, K. C. Younge, D. N. Matsukevich, L.-M. Duan, and C. Monroe, Entanglement of single-atom quantum bits at a distance, Nature (London) **449**, 68 (2007).

[6] S. Ritter, C. Nölleke, C. Hahn, A. Reiserer, A. Neuzner, M. Uphoff, M. Mücke, E. Figueroa, J. Bochmann, and G. Rempe, An elementary quantum network of single atoms in optical cavities, Nature (London) **484**, 195 (2012).

[7] B. Hensen, H. Bernien, A. E. Dreau, A. Reiserer, N. Kalb, M. S. Blok, J. Ruitenbern, R. F. L. Vermeulen, R. N. Schouten, C. Abellan, W. Amaya, V. Pruneri, M. W. Mitchell, M. Markham, D. J. Twitchen, D. Elkouss, S. Wehner, T. H. Taminiau, and R. Hanson, Loophole-free Bell inequality violation using electronic spins separated by 1.3 kilometers, Nature (London) **526**, 682 (2015).

[8] R. Riedinger, A. Wallucks, I. Marinkovic, C. Löschnauer, M. Aspelmeyer, S. Hong, and S. Gröblacher, Remote quantum entanglement between two micromechanical oscillators, Nature (London) **556**, 473 (2018).

[9] P. Kurpiers, P. Magnard, T. Walter, B. Royer, M. Pechal, J. Heinsoo, Y. Salathe, A. Akin, S. Storz, J.-C. Besse, S. Gasparinetti, A. Blais, and A. Wallraff, Deterministic quantum state transfer and remote entanglement using microwave photons, Nature (London) **558**, 264 (2018).

[10] A. Bienfait, K. J. Satzinger, Y. Zhong, H.-S. Chang, M.-H. Chou, C. R. Conner, É. Dumur, J. Grebel, G. A. Peairs, R. G. Povey, and A. N. Cleland, Phonon-mediated quantum state transfer and remote qubit entanglement, Science **364**, 368 (2019).

[11] K. G. Fedorov, M. Renger, S. Pogorzalek, R. Di Candia, Q. Chen, Y. Nojiri, K. Inomata, Y. Nakamura, M. Partanen, A. Marx, R. Gross, and F. Deppe, Experimental quantum teleportation of propagating microwaves, Sci. Adv. **7**, abk0891 (2021).

[12] M. Pompili *et al.*, Realization of a multinode quantum network of remote solid-state qubits, Science **372**, 259 (2021).

[13] V. Krutyanskiy, M. Galli, V. Krcmarsky, S. Baier, D. A. Fioretto, Y. Pu, A. Mazloom, P. Sekatski, M. Canteri,

M. Teller, J. Schupp, J. Bate, M. Meraner, N. Sangouard, B. P. Lanyon, and T. E. Northup, Entanglement of trapped-ion qubits separated by 230 meters, Phys. Rev. Lett. **130**, 050803 (2023).

[14] R. Sahu, L. Qiu, W. Hease, G. Arnold, Y. Minoguchi, P. Rabl, and J. M. Fink, Entangling microwaves with optical light, Science **380**, 718 (2023).

[15] H. J. Carmichael, *Statistical Methods in Quantum Optics 2: Non-Classical Fields* (Springer, Berlin, 1999).

[16] B. Kraus and J. I. Cirac, Discrete entanglement distribution with squeezed light, Phys. Rev. Lett. **92**, 013602 (2004).

[17] M. Paternostro, W. Son, and M. S. Kim, Complete conditions for entanglement transfer, Phys. Rev. Lett. **92**, 197901 (2004).

[18] A. L. Grimsmo and A. Blais, Squeezing and quantum state engineering with Josephson travelling wave amplifiers, npj Quantum Inf. **3**, 20 (2017).

[19] N. Didier, J. Guillaud, S. Shankar, and M. Mirrahimi, Remote entanglement stabilization and concentration by quantum reservoir engineering, Phys. Rev. A **98**, 012329 (2018).

[20] J. You, Z. Liao, S.-W. Li, and M. S. Zubairy, Waveguide quantum electrodynamics in squeezed vacuum, Phys. Rev. A **97**, 023810 (2018).

[21] L. C. G. Govia, A. Lingenfelter, and A. A. Clerk, Stabilizing two-qubit entanglement with engineered synthetic squeezing, Phys. Rev. Res. **4**, 023010 (2022).

[22] J. Agustí, Y. Minoguchi, J. M. Fink, and P. Rabl, Long-distance distribution of qubit-qubit entanglement using Gaussian-correlated photonic beams, Phys. Rev. A **105**, 062454 (2022).

[23] G. S. Agarwal and R. P. Puri, Cooperative behavior of atoms irradiated by broadband squeezed light, Phys. Rev. A **41**, 3782 (1990).

[24] R. Gutiérrez-Jáuregui, A. Asenjo-Garcia, and G. S. Agarwal, Dissipative stabilization of dark quantum dimers via squeezed vacuum, Phys. Rev. Res. **5**, 013127 (2023).

[25] S. Zippilli, M. Paternostro, G. Adesso, and F. Illuminati, Entanglement replication in driven dissipative many-body systems, Phys. Rev. Lett. **110**, 040503 (2013).

[26] A. Pocklington, Y.-X. Wang, Y. Yanay, and A. A. Clerk, Stabilizing volume-law entangled states of fermions and qubit using local dissipation, Phys. Rev. B **105**, L140301 (2022).

[27] Z.-L. Xiang, S. Ashhab, J. Q. You, and F. Nori, Hybrid quantum circuits: Superconducting circuits interacting with other quantum systems, Rev. Mod. Phys. **85**, 623 (2013).

[28] G. Kurizki, P. Bertet, Y. Kubo, K. Mølmer, D. Petrosyan, P. Rabl, and J. Schmiedmayer, Quantum technologies with hybrid systems, Proc. Natl. Acad. Sci. U.S.A. **112**, 3866 (2015).

[29] A. A. Clerk, K. W. Lehnert, P. Bertet, J. R. Petta, and Y. Nakamura, Hybrid quantum systems with circuit quantum electrodynamics, Nat. Phys. **16**, 257 (2020).

[30] X. Han, W. Fu, C.-L. Zou, L. Jiang, and H. X. Tang, Microwave-optical quantum frequency conversion, Optica **8**, 1050 (2021).

[31] J. P. Torres, K. Banaszek, and I. A. Walmsley, Engineering nonlinear optic sources of photonic entanglement, Prog. Opt. **56**, 227 (2011).

[32] C. Couteau, Spontaneous parametric down-conversion, Contemp. Phys. **59**, 291 (2018).

[33] C. Eichler, D. Bozyigit, C. Lang, M. Baur, L. Steffen, J. M. Fink, S. Filipp, and A. Wallraff, Observation of two-mode squeezing in the microwave frequency domain, Phys. Rev. Lett. **107**, 113601 (2011).

[34] E. P. Menzel, R. Di Candia, F. Deppe, P. Eder, L. Zhong, M. Ihmig, M. Haeberlein, A. Baust, E. Hoffmann, D. Ballester, K. Inomata, T. Yamamoto, Y. Nakamura, E. Solano, A. Marx, and R. Gross, Path entanglement of continuous-variable quantum microwaves, Phys. Rev. Lett. **109**, 250502 (2012).

[35] E. Flurin, N. Roch, F. Mallet, M. H. Devoret, and B. Huard, Generating entangled microwave radiation over two transmission lines, Phys. Rev. Lett. **109**, 183901 (2012).

[36] P. Winkel, I. Takmakov, D. Rieger, L. Planat, W. Hasch-Guichard, L. Grünhaupt, N. Maleeva, F. Foroughi, F. Henriques, K. Borisov, J. Ferrero, A. V. Ustinov, W. Wernsdorfer, N. Roch, and I. M. Pop, Nondegenerate parametric amplifiers based on dispersion-engineered Josephson-junction arrays, Phys. Rev. Appl. **13**, 024015 (2020).

[37] A. Peugeot, G. Menard, S. Dambach, M. Westig, B. Kubala, Y. Mukharsky, C. Altimiras, P. Joyez, D. Vion, P. Roche, D. Esteve, P. Milman, J. Leppäkangas, G. Johansson, M. Hofheinz, J. Ankerhold, and F. Portier, Generating two continuous entangled microwave beams using a dc-biased Josephson junction, Phys. Rev. X **11**, 031008 (2021).

[38] K. Stannigel, P. Rabl, and P. Zoller, Driven-dissipative preparation of entangled states in cascaded quantum-optical networks, New J. Phys. **14**, 063014 (2012).

[39] H. Pichler, T. Ramos, A. J. Daley, and P. Zoller, Quantum optics of chiral spin networks, Phys. Rev. A **91**, 042116 (2015).

[40] P. Lodahl, S. Mahmoodian, S. Stobbe, P. Schneeweiss, J. Volz, A. Rauschenbeutel, H. Pichler, and P. Zoller, Chiral quantum optics, Nature (London) **541**, 473 (2017).

[41] K. M. Sliwa, M. Hatridge, A. Narla, S. Shankar, L. Frunzio, R. J. Schoelkopf, and M. H. Devoret, Reconfigurable Josephson circulator/directional amplifier, Phys. Rev. X **5**, 041020 (2015).

[42] J. Kerckhoff, K. Lalumiere, B. J. Chapman, A. Blais, and K. W. Lehnert, On-chip superconducting microwave circulator from synthetic rotation, Phys. Rev. Appl. **4**, 034002 (2015).

[43] B. J. Chapman, E. I. Rosenthal, J. Kerckhoff, B. A. Moores, L. R. Vale, J. A. B. Mates, G. C. Hilton, K. Lalumiere, A. Blais, and K. W. Lehnert, Widely tunable on-chip microwave circulator for superconducting quantum circuits, Phys. Rev. X **7**, 041043 (2017).

[44] F. Lecocq, L. Ranzani, G. A. Peterson, K. Cicak, R. W. Simmonds, J. D. Teufel, and J. Aumentado, Nonreciprocal microwave signal processing with a field-programmable Josephson amplifier, Phys. Rev. Appl. **7**, 024028 (2017).

[45] S. Masuda, S. Kono, K. Suzuki, Y. Tokunaga, Y. Nakamura, and K. Koshino, Nonreciprocal microwave transmission based on Gebhard-Ruckenstein hopping, Phys. Rev. A **99**, 013816 (2019).

[46] Y.-Y. Wang, S. van Geldern, T. Connolly, Y.-X. Wang, A. Shilcusky, A. McDonald, A. A. Clerk, and C. Wang,

Low-loss ferrite circulator as a tunable chiral quantum system, Phys. Rev. Appl. **16**, 064066 (2021).

[47] P.-O. Guimond, B. Vermersch, M. L. Juan, A. Sharafiev, G. Kirchmair, and P. Zoller, A unidirectional on-chip photonic interface for superconducting circuits, npj Quantum Inf. **6**, 32 (2020).

[48] N. Gheeraert, S. Kono, and Y. Nakamura, Programmable directional emitter and receiver of itinerant microwave photons in a waveguide, Phys. Rev. A **102**, 053720 (2020).

[49] B. Kannan *et al.*, On-demand directional microwave photon emission using waveguide quantum electrodynamics, Nat. Phys. **19**, 394 (2023).

[50] C. Joshi, F. Yang, and M. Mirhosseini, Resonance fluorescence of a chiral artificial atom, Phys. Rev. X **13**, 021039 (2023).

[51] See Supplemental Material at http://link.aps.org/supplemental/10.1103/PhysRevLett.131.250801, which includes the additional Refs. [52–57], for more details on the derivation of the effective master equation, the uniqueness of the steady state, and additional numerical simulations.

[52] H. J. Carmichael, Quantum trajectory theory for cascaded open systems, Phys. Rev. Lett. **70**, 2273 (1993).

[53] C. W. Gardiner, Driving a quantum system with the output field from another driven quantum system, Phys. Rev. Lett. **70**, 2269 (1993).

[54] C. W. Gardiner and P. Zoller, *Quantum Noise* (Springer, Berlin, 2004).

[55] M. Esposito, A. Ranadive, L. Planat, and N. Roch, Perspective on traveling wave microwave parametric amplifiers, Appl. Phys. Lett. **119**, 120501 (2021).

[56] M. Esposito, A. Ranadive, L. Planat, S. Leger, D. Fraudet, V. Jouanny, O. Buisson, W. Guichard, C. Naud, J. Aumentado, F. Lecocq, and N. Roch, Observation of two-mode squeezing in a traveling wave parametric amplifier, Phys. Rev. Lett. **128**, 153603 (2022).

[57] J. A. Mlynek, A. A. Abdumalikov, C. Eichler, and A. Wallraff, Observation of Dicke superradiance for two artificial atoms in a cavity with high decay rate, Nat. Commun. **5**, 5186 (2014).

[58] S. Hill and W. K. Wootters, Entanglement of a pair of quantum bits, Phys. Rev. Lett. **78**, 5022 (1997).

[59] R. Horodecki, P. Horodecki, M. Horodecki, and K. Horodecki, Quantum entanglement, Rev. Mod. Phys. **81**, 865 (2009).

[60] B. Jungnitsch, T. Moroder, and O. Gühne, Taming multiparticle entanglement, Phys. Rev. Lett. **106**, 190502 (2011).

[61] C. Kruszynska and B. Kraus, Local entanglability and multipartite entanglement, Phys. Rev. A **79**, 052304 (2009).

[62] G. Vitagliano, A. Riera, and J. I. Latorre, Volume-law scaling for the entanglement entropy in spin-$1/2$ chains, New J. Phys. **12**, 113049 (2010).

[63] Z. Zhang, A. Ahmadain, and I. Klich, Novel quantum phase transition from bounded to extensive entanglement, Proc. Natl. Acad. Sci. U.S.A. **114**, 5142 (2017).

[64] A. Lingenfelter, M. Yao, A. Pocklington, Y.-X. Wang, A. Irfan, W. Pfaff, and A. A. Clerk, Exact results for a boundary-driven double spin chain and resource-efficient remote entanglement stabilization, arXiv:2307.09482.

[65] P. Magnard, S. Storz, P. Kurpiers, J. Schär, F. Marxer, J. Lütolf, T. Walter, J.-C. Besse, M. Gabureac, K. Reuer, A. Akin, B. Royer, A. Blais, and A. Wallraff, Microwave quantum link between superconducting circuits housed in spatially separated cryogenic systems, Phys. Rev. Lett. **125**, 260502 (2020).

[66] Y. Zhong, H.-S. Chang, A. Bienfait, E. Dumur, M.-H. Chou, C. R. Conner, J. Grebel, R. G. Povey, H. Yan, D. I. Schuster, and A. N. Cleland, Deterministic multi-qubit entanglement in a quantum network, Nature (London) **590**, 571 (2021).

[67] J. Niu *et al.*, Low-loss interconnects for modular superconducting quantum processors, Nat. Electron. **6**, 235 (2023).

[68] M. Renger, S. Gandorfer, W. Yam, F. Fesquet, M. Handschuh, K. E. Honasoge, F. Kronowetter, Y. Nojiri, M. Partanen, M. Pfeiffer, H. van der Vliet, A. J. Matthews, J. Govenius, R. N. Jabdaraghi, M. Prunnila, A. Marx, F. Deppe, R. Gross, and K. G. Fedorov, Cryogenic microwave link for quantum local area networks, arXiv:2308.12398.

[69] https://clip.science/.